Engineering of spontaneous emission in free space via conditional measurements

Manuel Bojer[1,*] Lukas Götzendörfer,[1] Romain Bachelard[2,3] and Joachim von Zanthier[1]

[1]*Institut für Optik, Information und Photonik, Universität Erlangen-Nürnberg, 91058 Erlangen, Germany*

[2]*Université Côte d'Azur, CNRS, Institut de Physique de Nice, 06560 Valbonne, France*

[3]*Departamento de Física, Universidade Federal de São Carlos, Rodovia Washington Luís, km 235-SP-310, 13565-905 São Carlos, São Paulo, Brazil*

(Received 5 April 2022; accepted 29 August 2022; published 11 October 2022)

We study the collective spontaneous emission of three identical two-level atoms initially prepared in the excited states by measuring Glauber's third-order photon correlation function. Assuming two atoms at subwavelength distance from each other such that they are subject to the dipole-dipole interaction while the third one is located several wavelengths away, we observe super- and subradiant decay alike, depending on the direction of observation. Unlike the case where no remote atom is introduced or no conditional measurements are performed, the spontaneous emission behavior of the conditioned three-atom system is strongly modified, i.e., differing from the single-atom and the canonical two-atom configuration. The conditional measurements associated with the three-photon correlation function in combination with the dipole-dipole interaction between the adjacent atoms lead to quantum interference among the different decay channels allowing one to engineer the spontaneous emission in space and time.

DOI: 10.1103/PhysRevResearch.4.043022

I. INTRODUCTION

The coupling of an excited atom to the electromagnetic vacuum field leads to deexcitation of the atom, a random process called spontaneous emission. A plethora of publications has discussed the possibilities to modify this fundamental process, e.g., by changing the properties of the vacuum field by use of cavities [1–5], by exploiting nano-optical devices [6–12], or applying external coherent fields [13,14]. Interestingly, an ensemble of interacting emitters in free space also leads to modified spontaneous emission, e.g., mediated by the dipole-dipole interaction [15], giving rise to collective spontaneous emission coined super- and subradiance [16–19].

The superradiant cascade from the fully excited state of an atomic ensemble to its ground state, where the system passes by the set of symmetric Dicke states with different decay rates, has been studied extensively in the past [17,18]. Recently, there has been renewed interest in the collective emission of atomic ensembles also in the single-excitation regime (sometimes labeled "single-photon" regime), where steady-state shifts [20–26] as well as superradiant [27–30] and subradiant [29–32] emission have been reported. The subradiant emission has been observed in particular in the late-time regime, after decoherence has eliminated the short-lived states and populated essentially the long-lived levels [33–35]. These works have in common that the radiation is typically monitored in a given direction, that is, all the photons are recorded within the same emission angle. In this way, only minor spatial modulations of the spontaneous emission rate have been observed, attributed to multiple scattering [27] or to linear dispersion [36].

In this work we show that a pronounced spatial modulation of the spontaneous emission rate can be obtained by combining dipole-dipole interactions among the emitters with conditional measurements of the scattered photons. We consider the simplest configuration where this phenomenon is observable, namely three atoms, where two of them are separated at subwavelength distance from each other, while the third one is located several wavelengths apart, all entangled via conditional photon measurement [30,37–44]. In this configuration, the strong dipole-dipole interaction between the adjacent atoms leads to a marked modification of the spontaneous decay rate of the two emitters [16]; this rate is, however, almost isotropic due to their close separation. The decay rate becomes modulated in space only due to the presence of the remote atom, entangled with the other two atoms. By measuring Glauber's third-order photon correlation function where two photons are initially recorded in given directions, all three atoms become entangled giving rise to spatially varying quantum interferences among the different decay channels of the three atoms. In this case a modulated spatial pattern for the emission rate of the last photon is obtained, displaying both superradiant and subradiant decay. Note that a two-atom system cannot support both a strong modification of the spontaneous emission rate (obtained for close atoms) and a spatial modulation (accessible only with remote atoms). Our work thus paves the way for engineering the photon emission rate by taking advantage of both dipole-dipole interactions and distant atom-atom correlations.

*manuelbojer6@gmail.com

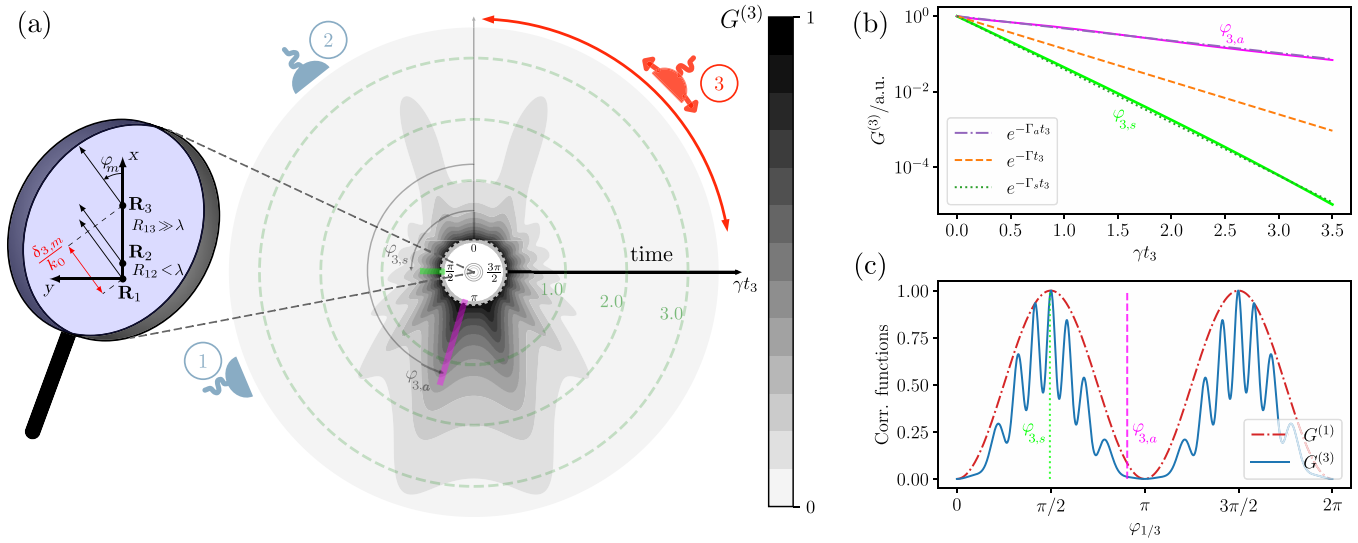

FIG. 1. (a) Three identical two-level atoms placed at $\boldsymbol{R}_1 = \boldsymbol{0}$, $\boldsymbol{R}_2 = \lambda/3\hat{\boldsymbol{x}}$, and $\boldsymbol{R}_3 = 4\lambda\hat{\boldsymbol{x}}$ along the x axis; with $R_{12} < \lambda$, the first two atoms are subject to the dipole-dipole interaction, while the third atom, with $R_{23} \gg \lambda$, is not. Starting from the fully excited state, the three-atom system is projected onto an entangled state via the measurement of two photons at space-time points $(\varphi_1 = 2\pi/3, t_1 = 0)$ and $(\varphi_2 = \pi/4.4, t_2 = 0)$ (blue detectors). The signal of the third detector (red) then corresponds to the probability to record the last photon at space-time point (φ_3, t_3), collectively scattered by the entangled atomic ensemble. The contour plot shows the third-order photon correlation function $G^{(3)}(\varphi_3, t_3)$, normalized for each direction by its initial value; angles $\varphi_{3,s} \approx 1.56$ $(\varphi_{3,a} \approx 2.85)$ indicate the directions at which an effective superradiant (subradiant) decay is observed. (b) Time evolution of $G^{(3)}(\varphi_3, t_3)$, normalized by its value at time zero, for the two directions $\varphi_{3,s}$ (thick lime line) and $\varphi_{3,a}$ (thin magenta line), where the decay rate is approximately given by the symmetric $\Gamma_s = 2(\gamma + \Delta\gamma)$ and antisymmetric $\Gamma_a = 2(\gamma - \Delta\gamma)$ decay rate, respectively; the dash-dotted purple, dashed orange, and dotted green lines are exponential curves displaying the antisymmetric, single atom, and symmetric decay rates, respectively. (c) Third-order correlation function $G^{(3)}(\varphi_3, t_3 = 0)$ (blue solid curve) and first-order correlation function $G^{(1)}(\varphi_1, t_1 = 0)$ (red dash-dotted curve) at initial times; the entanglement of the three-atom system created by the measurement of the first two photons leads to a strong modulation in space of $G^{(3)}(\varphi_3, t_3 = 0)$, whereas $G^{(1)}(\varphi_1, t_1 = 0)$ displays only the dipole radiation pattern; the direction at which an effective superradiant (subradiant) decay is observed is indicated by the dotted lime (dashed magenta) line.

II. TIME EVOLUTION - QUANTUM MASTER EQUATION

We start by investigating the emission dynamics by use of the master equation for three identical two-level atoms. To demonstrate the effect, it is sufficient to restrict the analysis to three atoms located at positions $\boldsymbol{R}_\mu = (x_\mu, y_\mu)$, $\mu \in \{1, 2, 3\}$ within the xy plane, as illustrated in Fig. 1(a). Here, two atoms are assumed to be adjacent with subwavelength separation such that they are subject to the dipole-dipole interaction, while the third atom is located at a distance of several wavelengths from the other two emitters, so that the light-mediated interaction with the first two atoms can be neglected. The state of the atomic system is conveniently expressed using the collective Dicke basis for the first two atoms,

$$
\begin{aligned}
|E\rangle &= |e, e\rangle\,, \quad |G\rangle = |g, g\rangle\,,\\
|S\rangle &= \frac{1}{\sqrt{2}}(|e, g\rangle + |g, e\rangle),\\
|A\rangle &= \frac{1}{\sqrt{2}}(|e, g\rangle - |g, e\rangle),
\end{aligned}
\tag{1}
$$

and the bare atomic basis with excited state $|e\rangle$ and ground state $|g\rangle$ for the remaining third atom. In this case, the master equation for the three-atom density matrix $\hat{\rho}$ reads [17,45]

$$
\begin{aligned}
\partial_t \hat{\rho} = &-i\omega_0 \sum_{\mu=1}^{3} \big[\hat{S}_z^{(\mu)}, \hat{\rho}\big] + i \sum_{\substack{\mu,\nu=1\\ \mu\neq\nu}}^{2} \Delta\Omega[\hat{S}_+^{(\mu)}\hat{S}_-^{(\nu)}, \hat{\rho}]\\
&- \sum_{\mu=1}^{3} \gamma(\hat{S}_+^{(\mu)}\hat{S}_-^{(\mu)}\hat{\rho} - 2\hat{S}_-^{(\mu)}\hat{\rho}\hat{S}_+^{(\mu)} + \hat{\rho}\hat{S}_+^{(\mu)}\hat{S}_-^{(\mu)})\\
&- \sum_{\substack{\mu,\nu=1\\ \mu\neq\nu}}^{2} \Delta\gamma(\hat{S}_+^{(\mu)}\hat{S}_-^{(\nu)}\hat{\rho} - 2\hat{S}_-^{(\nu)}\hat{\rho}\hat{S}_+^{(\mu)} + \hat{\rho}\hat{S}_+^{(\mu)}\hat{S}_-^{(\nu)}).
\end{aligned}
\tag{2}
$$

Here, $\hat{S}_+^{(\mu)}$ $(\hat{S}_-^{(\mu)})$ denotes the raising (lowering) operator of the μth atom and $\hat{S}_z^{(\mu)} = \frac{1}{2}(\hat{S}_+^{(\mu)}\hat{S}_-^{(\mu)} - \hat{S}_-^{(\mu)}\hat{S}_+^{(\mu)})$. Moreover, $\omega_0 = k_0 c = 2\pi c/\lambda$ stands for the atomic transition frequency and $\Gamma = 2\gamma$ the single atom decay rate, whereas the coupling parameters $\Delta\gamma$ and $\Delta\Omega$ account for the dipole-dipole interaction between the first two atoms

$$
\begin{aligned}
\Delta\Omega - i\Delta\gamma = \frac{3}{2}\gamma\, e^{-ik_0 R_{12}} \Bigg[&\frac{1 - \cos^2\psi}{k_0 R_{12}}\\
&- [1 - 3\cos^2\psi]\left(\frac{i}{(k_0 R_{12})^2} + \frac{1}{(k_0 R_{12})^3}\right)\Bigg],
\end{aligned}
\tag{3}
$$

with $R_{12} = |\boldsymbol{R}_{12}| = |\boldsymbol{R}_1 - \boldsymbol{R}_2|$ and ψ the angle between the atomic dipole moment $\boldsymbol{d}$ and $\boldsymbol{R}_{12}$.

III. THIRD-ORDER PHOTON CORRELATION FUNCTION

We assume the system to be initially in the fully excited state $|E, e\rangle$. To calculate the third-order photon correlation function, we assume that two detectors at $\boldsymbol{r}_1$ and $\boldsymbol{r}_2$ record two photons spontaneously emitted by the three-atom system at time $t_1 = t_2 = 0$, whereas the third photon is measured at position $\boldsymbol{r}_3$ at time t_3. The detection of a photon corresponds to the annihilation of the light particle, described by the positive frequency part of the electric field operator $\hat{\boldsymbol{E}}_m^{(+)}$ (with $\hat{\boldsymbol{E}}_m^{(-)} = [\hat{\boldsymbol{E}}_m^{(+)}]^\dagger$). Calling $\hat{\boldsymbol{r}}_m = \boldsymbol{r}_m/r_m = \hat{\boldsymbol{x}}\cos\varphi_m + \hat{\boldsymbol{y}}\sin\varphi_m$ the direction of the detector in the far field we can write

$$\hat{\boldsymbol{E}}_m^{(+)} \propto \hat{\boldsymbol{r}}_m \times (\hat{\boldsymbol{r}}_m \times \boldsymbol{d}) \cdot \sum_{\mu=1}^{3} e^{i\delta_{\mu,m}} \hat{S}_-^{(\mu)}, \tag{4}$$

where the cross product yields the usual dipole radiation pattern. In addition, the phase

$$\delta_{\mu,m} = -k_0 \boldsymbol{R}_\mu \cdot \hat{\boldsymbol{r}}_m = -k_0[x_\mu \cos\varphi_m + y_\mu \sin\varphi_m] \tag{5}$$

accounts for the relative geometric phase (or optical path) accumulated by a photon when propagating from the emitter at $\boldsymbol{R}_\mu$ to the detector at $\boldsymbol{r}_m$ relative to a photon emitted at the origin [see Fig. 1(a)].

Considering the fully excited state Glauber's third-order photon correlation function, i.e., the conditional probability to record a photon at the third detector at space-time point $(\boldsymbol{r}_3, t_3)$ given that two photons have been measured at $(\boldsymbol{r}_2, 0)$ and $(\boldsymbol{r}_1, 0)$, we find [46–48]

$$G^{(3)}(\boldsymbol{r}_1, \boldsymbol{r}_2, \boldsymbol{r}_3; 0, 0, t_3) = \langle \hat{\boldsymbol{E}}_1^{(-)} \hat{\boldsymbol{E}}_2^{(-)} \hat{\boldsymbol{E}}_3^{(-)} \hat{\boldsymbol{E}}_3^{(+)} \hat{\boldsymbol{E}}_2^{(+)} \hat{\boldsymbol{E}}_1^{(+)} \rangle_{|E,e\rangle\langle E,e|}. \tag{6}$$

Without loss of generality, we can set $\boldsymbol{R}_1 = (0, 0)$ leading to [48]

$$\begin{aligned} G^{(3)}(\boldsymbol{r}_3, t_3) \propto\ & \sin^2(\alpha)[|c_{Ge}|^2 e^{-2\gamma t_3} + 2|c_{Sg}|^2 e^{-2(\gamma+\Delta\gamma)t_3} \cos^2(\delta_{2,3}/2) + 2|c_{Ag}|^2 e^{-2(\gamma-\Delta\gamma)t_3} \sin^2(\delta_{2,3}/2) \\ & + 2|c_{Sg}||c_{Ag}| e^{-2\gamma t_3} \sin(\delta_{2,3}) \sin(\varphi_{Ag} - \varphi_{Sg} - 2\,\Delta\Omega\, t_3) \\ & + 2\sqrt{2}|c_{Sg}||c_{Ge}| e^{-(2\gamma+\Delta\gamma)t_3} \cos(\delta_{2,3}/2) \cos(\varphi_{Sg} + \delta_{2,3}/2 - \delta_{3,3} + \Delta\Omega\, t_3) \\ & + 2\sqrt{2}|c_{Ag}||c_{Ge}| e^{-(2\gamma-\Delta\gamma)t_3} \sin(\delta_{2,3}/2) \sin(\varphi_{Ag} + \delta_{2,3}/2 - \delta_{3,3} - \Delta\Omega\, t_3)], \end{aligned} \tag{7}$$

where the coefficients c_{Ge}, c_{Sg}, and c_{Ag} read (see also the discussion on the two-photon subtracted state in [48])

$$\begin{aligned} c_{Ge} &= (e^{i\delta_{2,1}} + e^{i\delta_{2,2}}), \\ c_{Sg} &= \frac{1}{\sqrt{2}}(e^{i(\delta_{3,1}+\delta_{2,2})} + e^{i(\delta_{2,1}+\delta_{3,2})} + e^{i\delta_{3,1}} + e^{i\delta_{3,2}}), \\ c_{Ag} &= \frac{1}{\sqrt{2}}(e^{i(\delta_{3,1}+\delta_{2,2})} + e^{i(\delta_{2,1}+\delta_{3,2})} - e^{i\delta_{3,1}} - e^{i\delta_{3,2}}), \end{aligned} \tag{8}$$

and the phases associated with the complex coefficients c_{Sg} and c_{Ag} are given by $\varphi_{Sg/Ag} = \mathrm{Arg}(\frac{c_{Sg/Ag}}{c_{Ge}})$. In Eq. (7), the $\sin^2(\alpha)$ term accounts for the dipole radiation pattern, with α the angle between the direction of the last detector $\hat{\boldsymbol{r}}_3$ and the dipole moment $\boldsymbol{d}$ of the atoms.

IV. SPATIAL INTERFERENCE PATTERNS

In what follows, we place the three atoms along the x axis and assume the dipole moment to be parallel to this axis, $\boldsymbol{d} = d\hat{\boldsymbol{x}}$, such that $\alpha = \varphi_3$ [see Fig. 1(a)]. The spatial and temporal behavior of $G^{(3)}(\boldsymbol{r}_3, t_3)$ is thus tuned by the six geometrical phases $\delta_{\mu,m}$, $\mu \in \{2, 3\}$ [with $\boldsymbol{R}_1 = (0, 0)$] and $m \in \{1, 2, 3\}$. This large parameter space results in a great variety of atom geometries, state preparation, and detection setups, each with different outcome for $G^{(3)}(\boldsymbol{r}_3, t_3)$. For example, the specific cases $|c_{Sg}| = 0$ or $|c_{Ag}| = 0$ reveal regimes in which $G^{(3)}(t_3)$ strongly deviates from a true exponential decay and rather presents either a global maximum or a true root $G^{(3)}(t_3) = 0$ at finite time $t_3 > 0$, corresponding to birth and death of spontaneous emission, respectively [48].

If the three atoms are placed at $\boldsymbol{R}_1 = \boldsymbol{0}$, $\boldsymbol{R}_2 = \lambda/3\hat{\boldsymbol{x}}$, and $\boldsymbol{R}_3 = 4\lambda\hat{\boldsymbol{x}}$ and the first two photon detection events at time zero occur in space at $\varphi_1 = 2\pi/3$ and $\varphi_2 = \pi/4.4$, then Glauber's third-order correlation function $G^{(3)}(\boldsymbol{r}_3, t_3)$, normalized for each direction φ_3 by its value at time zero, takes the form shown in Fig. 1(a). In this case, both super- and subradiant decay can be observed along certain directions simultaneously, i.e., depending only on the position of the third detector, as illustrated in Fig. 1(b). We note that one can also find positions of the first two detectors for which one can observe solely either superradiant or subradiant decay for particular positions of the third detector. We further emphasize that similar emission patterns as the one shown in Fig. 1(a) can be found for other positions of the first two detectors, allowing one to engineer the spontaneous emission of the three-atom system in a similar manner. We finally note that the emission dynamics in each direction results from the sum of different modes [see Eq. (7)].

This variety of decay rates in space comes with a rich spatial interference pattern of $G^{(3)}(\boldsymbol{r}_3, t_3 = 0)$ exhibiting a series of fringes [Fig. 1(c)]. The pattern stems from the quantum interference of the emission probability of the remote atom with that of the other two emitters, with the latter two being too close to produce a spatial modulation on their own. The number of fringes is directly related to the distance of the third atom to the other two atoms, i.e., putting it farther away will increase that number.

We highlight that this great variety of modified spontaneous emission in both space and time results from the combined action of dipole-dipole interaction and conditional

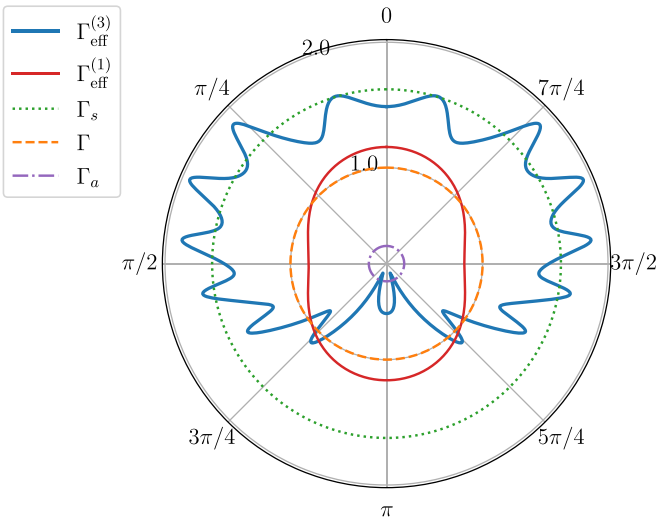

FIG. 2. Effective decay rate $\Gamma^{(3)}_{\text{eff}}$ of the third-order photon correlation function $G^{(3)}(\varphi_3, t_3)$ as a function of the direction of observation (thick blue solid curve), together with the effective decay rate $\Gamma^{(1)}_{\text{eff}}$ of the intensity measurement $G^{(1)}(\varphi_1, t_1)$ (red solid line), the symmetric decay rate $\Gamma_s = 2(\gamma + \Delta\gamma)$ (green dotted line), the single-atom decay rate Γ (orange dashed line), and the antisymmetric decay rate $\Gamma_a = 2(\gamma - \Delta\gamma)$ (purple dash-dotted line) for the same setup as in Fig. 1. The effective decay rates, all presented in units of γ, are calculated by an exponential fit of the correlation functions in the time interval $\gamma t \in [0, 0.5]$.

measurements leading to entanglement of the sources. Indeed, although one may argue that interference of the light fields among the three emitters occurs independently of the conditional measurement intrinsic to $G^{(3)}(\boldsymbol{r}_3, t_3)$, i.e., leaving aside the conditional measurements, alters the emission pattern drastically. This is due to the fact that the states responsible for the light emission are very different in both cases. While only an isotropic emission pattern is obtained for $G^{(1)}(\boldsymbol{r}_1, t_1 = 0)$ starting from the state $|E, e\rangle$ [up to the dipole radiation pattern $\sin^2(\alpha)$], $G^{(3)}(\boldsymbol{r}_3, t_3 = 0)$ displays strong spatial modulations. In Fig. 1(c), the emission patterns obtained from Glauber's first- and third-order correlation functions are presented. As can be seen, the superposition of the light fields from the two close atoms with the one of the remote atom fails to produce the intricate fringe pattern produced by the three-atom system entangled via the conditional measurements [49].

V. DIRECTIONAL DECAY RATES

Moreover, a careful analysis of the emission dynamics reveals how the entanglement of the atoms affects also the temporal emission properties of the three-atom system. In Fig. 2 (thick blue solid curve) the effective decay rates of $G^{(3)}(\boldsymbol{r}_3, t_3)$ are computed for different directions of observation for the same conditional measurement configuration as in Fig. 1. The decay rates are obtained by fitting exponentially the radiation dynamics of $G^{(3)}(\boldsymbol{r}_3, t_3)$ in the time interval $\gamma t \in [0, 0.5]$. We note, however, that in general the emission pattern results from a superposition of different modes leading not to a simple exponential decay but rather to a superposition of exponential decays or even to mode beating and an oscillatory behavior. Therefore, an exponential fit to obtain the effective decay rates is only viable in the early time dynamics. Yet, the emission from the entangled states associated with a $G^{(3)}$ measurement in fact *allows* all three modes (symmetric, antisymmetric, and single atom) to contribute to the temporal emission behavior, thus producing the intricate pattern of effective decay rates displayed in Figs. 1(a) and 2. The latter is in strong contrast to the pattern obtained by a direct measurement of the decaying intensity $G^{(1)}$, i.e., obtained without conditional measurement, leading merely to a weak modulation of the decay rate in space as shown in Fig. 2 (red solid curve). This modulation results only from the interference between the emission of the first two atoms.

We note that, while the dipole-dipole interaction between two atoms allows for modifications of the decay rate which are either larger or smaller than the single-atom decay rate [i.e., the signatures of super- and subradiance as in Eq. (3)], $G^{(3)}(\boldsymbol{r}_3, t_3)$ displays a multitude of directions with faster-than-symmetric and slower-than-antisymmetric decay rates (see Fig. 2). Indeed, the coherent part of the dipole-dipole interaction leads to frequency shifts of the collective modes and eventually mode beating since the different modes contributing to the radiation in Eq. (7) compete. The obtained oscillations result in an increase or decrease of the decay rates at initial times [48], surpassing the symmetric and antisymmetric decay rate in certain directions.

We end by noting that the conditional measurements, i.e., the necessity to select photons with specific properties, inevitably lead to a limited efficiency, since only a small part of the total emitted power fulfills these requirements. However, recent experiments have shown that our proposals can be implemented in realistic setups [50,51]. Our study rather aims to investigate the conditions of a system allowing one to design the spontaneous emission properties in specific directions, based on dipole-dipole interactions and quantum interference.

VI. CONCLUSION

In conclusion, we demonstrated how conditional measurements combined with dipole-dipole interactions enable manipulation and even engineering of the spontaneous emission behavior, both in space and time, of an atomic ensemble. Dipole-dipole interactions are strongest for subwavelength samples [16], from which, however, no appreciable interference pattern is obtained. Imposing correlations between remote atoms by conditional measurements allows one to bypass this restriction of short interatomic distances; this becomes an option because the generation of entanglement via conditional measurements is possible even for remote atoms [49,52]. In this work, we have shown how to combine these two atom-correlating processes within the simplest configuration, i.e., using a pair of close atoms correlated to a remote one by conditional measurement.

The marked quantum interference resulting from the conditional measurements reveals directions along which subradiant decay dominates the emission, from the earliest moment and at odds from the two-atom case [48]. However, it should be mentioned that in the three-atom case, congruent to the two-atom case, the subradiant mode scales in the small-distance limit as $c_{Ag} \propto R_{12}/\lambda$. Thus increasing the lifetime of the subradiant mode goes along with a decrease in the corresponding population. In the future, we will investigate how subsequent conditional measurements in space *and* time will modify the collective decay and how the behavior scales with increasing number of emitters. This work shows that collective spontaneous emission is a rich line of research with unexpected outcomes beyond the canonical two-atom case, even if only a single atom is added to the system.

ACKNOWLEDGMENTS

M.B. and L.G. gratefully acknowledge funding and support by the International Max Planck Research School, Physics of Light. R.B. and J.v.Z. gratefully acknowledge funding and support by the Bavarian Academic Center for Latin America (BAYLAT). This work was funded by the Deutsche Forschungsgemeinschaft (DFG, German Research Foundation), Project-ID No. 429529648, TRR 306 QuCoLiMa ("Quantum Cooperativity of Light and Matter"). R.B. is supported by the São Paulo Research Foundation (FAPESP, Grants No. 2018/15554-5 and No. 2019/13143-0) and by the Brazilian National Council for Scientific and Technological Development (CNPq, Grants No. 313886/2020-2 and No. 409946/2018-4).

[1] E. M. Purcell, H. C. Torrey, and R. V. Pound, Resonance absorption by nuclear magnetic moments in a solid, Phys. Rev. **69**, 37 (1946).

[2] D. Kleppner, Inhibited Spontaneous Emission, Phys. Rev. Lett. **47**, 233 (1981).

[3] G. S. Agarwal, Quantum electrodynamics in the presence of dielectrics and conductors. IV. General theory for spontaneous emission in finite geometries, Phys. Rev. A **12**, 1475 (1975).

[4] P. Goy, J. M. Raimond, M. Gross, and S. Haroche, Observation of Cavity-Enhanced Single-Atom Spontaneous Emission, Phys. Rev. Lett. **50**, 1903 (1983).

[5] J. Eschner, C. Raab, F. Schmidt-Kaler, and R. Blatt, Light interference from single atoms and their mirror images, Nature (London) **413**, 495 (2001).

[6] P. Lodahl, S. Mahmoodian, S. R. Stobbe, A. Rauschenbeutel, P. Schneeweiss, J. Volz, H. Pichler, and P. Zoller, Chiral quantum optics, Nature (London) **541**, 473 (2017).

[7] D. E. Chang, J. S. Douglas, A. González-Tudela, C.-L. Hung, and H. J. Kimble, Colloquium: Quantum matter built from nanoscopic lattices of atoms and photons, Rev. Mod. Phys. **90**, 031002 (2018).

[8] A. Sipahigil, R. E. Evans, D. D. Sukachev, M. J. Burek, J. Borregaard, M. K. Bhaskar, C. T. Nguyen, J. L. Pacheco, H. A. Atikian, C. Meuwly, R. M. Camacho, F. Jelezko, E. Bielejec, H. Park, M. Lončar, and M. D. Lukin, An integrated diamond nanophotonics platform for quantum-optical networks, Science **354**, 847 (2016).

[9] R. E. Evans, M. K. Bhaskar, D. D. Sukachev, C. T. Nguyen, A. Sipahigil, M. J. Burek, B. Machielse, G. H. Zhang, A. S. Zibrov, E. Bielejec, H. Park, M. Lonar, and M. D. Lukin, Photon-mediated interactions between quantum emitters in a diamond nanocavity, Science **362**, 662 (2018).

[10] J.-H. Kim, S. Aghaeimeibodi, C. J. K. Richardson, R. P. Leavitt, and E. Waks, Super-radiant emission from quantum dots in a nanophotonic waveguide, Nature (London) **18**, 4734 (2018).

[11] J. Q. Grim, A. S. Bracker, M. Zalalutdinov, S. G. Carter, A. C. Kozen, M. Kim, C. S. Kim, J. T. Mlack, M. Yakes, B. Lee, and D. Gammon, Scalable in operando strain tuning in nanophotonic waveguides enabling three-quantum-dot superradiance, Nat. Mater. **18**, 963 (2019).

[12] A. S. Prasad, J. Hinney, S. Mahmoodian, K. Hammerer, S. Rind, P. Schneeweiss, A. S. Sõrensen, J. Volz, and A. Rauschenbeutel, Correlating photons using the collective nonlinear response of atoms weakly coupled to an optical mode, Nat. Photon. **14**, 719 (2020).

[13] S.-Y. Zhu and M. O. Scully, Spectral Line Elimination and Spontaneous Emission Cancellation via Quantum Interference, Phys. Rev. Lett. **76**, 388 (1996).

[14] E. Paspalakis and P. L. Knight, Phase Control of Spontaneous Emission, Phys. Rev. Lett. **81**, 293 (1998).

[15] R. H. Lehmberg, Radiation from an n-atom system. I. General formalism, Phys. Rev. A **2**, 883 (1970).

[16] R. H. Dicke, Coherence in spontaneous radiation processes, Phys. Rev. **93**, 99 (1954).

[17] G. S. Agarwal, in *Quantum Statistical Theories of Spontaneous Emission and Their Relation to Other Approaches—Quantum Optics*, edited by G. Höhler (Springer-Verlag, Berlin, 1974).

[18] M. Gross and S. Haroche, Superradiance: An essay on the theory of collective spontaneous emission, Phys. Rep. **93**, 301 (1982).

[19] Z. Ficek and R. Tanaś, Entangled states and collective nonclassical effects in two-atom systems, Phys. Rep. **372**, 369 (2002).

[20] T. Ido, T. H. Loftus, M. M. Boyd, A. D. Ludlow, K. W. Holman, and J. Ye, Precision Spectroscopy and Density-Dependent Frequency Shifts in Ultracold Sr, Phys. Rev. Lett. **94**, 153001 (2005).

[21] M. O. Scully and A. A. Svidzinsky, The effects of the n atom collective lamb shift on single photon superradiance, Phys. Lett. A **373**, 1283 (2009).

[22] J. Keaveney, A. Sargsyan, U. Krohn, I. G. Hughes, D. Sarkisyan, and C. S. Adams, Cooperative Lamb Shift in an Atomic Vapor Layer of Nanometer Thickness, Phys. Rev. Lett. **108**, 173601 (2012).

[23] J. Javanainen, J. Ruostekoski, Y. Li, and S.-M. Yoo, Shifts of a Resonance Line in a Dense Atomic Sample, Phys. Rev. Lett. **112**, 113603 (2014).

[24] Z. Meir, O. Schwartz, E. Shahmoon, D. Oron, and R. Ozeri, Cooperative Lamb Shift in a Mesoscopic Atomic Array, Phys. Rev. Lett. **113**, 193002 (2014).

[25] S. Jennewein, M. Besbes, N. J. Schilder, S. D. Jenkins, C. Sauvan, J. Ruostekoski, J.-J. Greffet, Y. R. P. Sortais, and A.

Browaeys, Coherent Scattering of Near-Resonant Light by a Dense Microscopic Cold Atomic Cloud, Phys. Rev. Lett. **116**, 233601 (2016).

[26] S. L. Bromley, B. Zhu, M. Bishof, X. Zhang, T. Bothwell, J. Schachenmayer, T. L. Nicholson, R. Kaiser, S. F. Yelin, M. D. Lukin, A. M. Rey, and J. Ye, Collective atomic scattering and motional effects in a dense coherent medium, Nat. Commun. **7**, 11039 (2016).

[27] M. O. Araújo, I. Krešić, R. Kaiser, and W. Guerin, Superradiance in a Large and Dilute Cloud of Cold Atoms in the Linear-Optics Regime, Phys. Rev. Lett. **117**, 073002 (2016).

[28] S. J. Roof, K. J. Kemp, M. D. Havey, and I. M. Sokolov, Observation of Single-Photon Superradiance and the Cooperative Lamb Shift in an Extended Sample of Cold Atoms, Phys. Rev. Lett. **117**, 073003 (2016).

[29] G. Araneda, D. B. Higginbottom, L. Slodička, Y. Colombe, and R. Blatt, Interference of Single Photons Emitted by Entangled Atoms in Free Space, Phys. Rev. Lett. **120**, 193603 (2018).

[30] S. Richter, S. Wolf, J. von Zanthier, and F. Schmidt-Kaler, Collective photon emission patterns from two atoms in free space, arXiv:2202.13678.

[31] W. Guerin, M. O. Araújo, and R. Kaiser, Subradiance in a Large Cloud of Cold Atoms, Phys. Rev. Lett. **116**, 083601 (2016).

[32] D. Das, B. Lemberger, and D. D. Yavuz, Subradiance and superradiance-to-subradiance transition in dilute atomic clouds, Phys. Rev. A **102**, 043708 (2020).

[33] A. Cipris, N. A. Moreira, T. S. do Espirito Santo, P. Weiss, C. J. Villas-Boas, R. Kaiser, W. Guerin, and R. Bachelard, Subradiance with Saturated Atoms: Population Enhancement of the Long-Lived States, Phys. Rev. Lett. **126**, 103604 (2021).

[34] G. Ferioli, A. Glicenstein, L. Henriet, I. Ferrier-Barbut, and A. Browaeys, Storage and Release of Subradiant Excitations in a Dense Atomic Cloud, Phys. Rev. X **11**, 021031 (2021).

[35] A. C. dos Santos, A. Cidrim, C. J. Villas-Boas, R. Kaiser, and R. Bachelard, Generating long-lived entangled states with free-space collective spontaneous emission, Phys. Rev. A **105**, 053715 (2022).

[36] A. S. Kuraptsev, I. M. Sokolov, and M. D. Havey, Angular distribution of single-photon superradiance in a dilute and cold atomic ensemble, Phys. Rev. A **96**, 023830 (2017).

[37] C. Cabrillo, J. I. Cirac, P. García-Fernández, and P. Zoller, Creation of entangled states of distant atoms by interference, Phys. Rev. A **59**, 1025 (1999).

[38] C. Skornia, J. von Zanthier, G. S. Agarwal, E. Werner, and H. Walther, Nonclassical interference effects in the radiation from coherently driven uncorrelated atoms, Phys. Rev. A **64**, 063801 (2001).

[39] D. E. Browne, M. B. Plenio, and S. F. Huelga, Robust Creation of Entanglement between Ions in Spatially Separate Cavities, Phys. Rev. Lett. **91**, 067901 (2003).

[40] D. L. Moehring, P. Maunz, S. Olmschenk, K. C. Younge, D. N. Matsukevich, L.-M. Duan, and C. Monroe, Entanglement of single-atom quantum bits at a distance, Nature (London) **449**, 68 (2007).

[41] J. Hofmann, M. Krug, N. Ortegel, L. Gérard, M. Weber, W. Rosenfeld, and H. Weinfurter, Heralded entanglement between widely separated atoms, Science **337**, 72 (2012).

[42] L. Slodička, G. Hétet, N. Röck, P. Schindler, M. Hennrich, and R. Blatt, Atom-Atom Entanglement by Single-Photon Detection, Phys. Rev. Lett. **110**, 083603 (2013).

[43] H. Bernien, B. Hensen, W. Pfaff, G. Koolstra, M. S. Blok, L. Robledo, T. Taminiau, M. Markham, D. J. Twitchen, L. Childress, and R. Hanson, Heralded entanglement between solid-state qubits separated by three metres, Nature (London) **497**, 86 (2013).

[44] A. Delteil, Z. Sun, W.-B. Gao, E. Togan, S. Faelt, and A. Imamoğlu, Generation of heralded entanglement between distant hole spins, Nat. Phys. **12**, 218 (2016).

[45] Z. Ficek and S. Swain, *Quantum Interference and Coherence: Theory and Experiments* (Springer-Verlag, Berlin, 2005).

[46] S. Oppel, R. Wiegner, G. S. Agarwal, and J. von Zanthier, Directional Superradiant Emission from Statistically Independent Incoherent Nonclassical and Classical Sources, Phys. Rev. Lett. **113**, 263606 (2014).

[47] R. Wiegner, S. Oppel, D. Bhatti, J. von Zanthier, and G. S. Agarwal, Simulating superradiance from higher-order-intensity-correlation measurements: Single atoms, Phys. Rev. A **92**, 033832 (2015).

[48] S. Mährlein, L. Götzendörfer, K. Günthner, J. Evers, and J. von Zanthier, Birth, death, and revival of spontaneous emission in a three-atom system, Phys. Rev. Res. **2**, 013278 (2020).

[49] C. Thiel, J. von Zanthier, T. Bastin, E. Solano, and G. S. Agarwal, Generation of Symmetric Dicke States of Remote Qubits with Linear Optics, Phys. Rev. Lett. **99**, 193602 (2007).

[50] S. Wolf, S. Richter, J. von Zanthier, and F. Schmidt-Kaler, Light of Two Atoms in Free Space: Bunching or Antibunching? Phys. Rev. Lett. **124**, 063603 (2020).

[51] S. Richter, S. Wolf, J. von Zanthier, and F. Schmidt-Kaler, Imaging Trapped Ion Structures via Fluorescence Cross-Correlation Detection, Phys. Rev. Lett. **126**, 173602 (2021).

[52] T. Bastin, C. Thiel, J. von Zanthier, L. Lamata, E. Solano, and G. S. Agarwal, Operational Determination of Multiqubit Entanglement Classes via Tuning of Local Operations, Phys. Rev. Lett. **102**, 053601 (2009).